Star Formation at High Angular Resolution
IAU Symposium, Vol. 221, 2004
M.G. Burton, R. Jayawardhana & T.L. Bourke, eds.

The Structures and Kinematics of Protoclusters

James Di Francesco
National Research Council of Canada, Herzberg Institute of Astrophysics, 5071 West Saanich Rd., Victoria, BC V9E 2E7 CANADA

Abstract. Embedded clusters produce the greatest numbers of stars within our Galaxy but the process by which clusters themselves form is not well understood. The structures and kinematics of the very youngest embedded clusters, i.e., "protoclusters" with ages $<10^6$ yr, should provide needed insight. To gauge their utility in this regard, we examine recent observations of a nearby protocluster in Ophiuchus. Near-infrared images of the Oph A core reveal numerous young objects but the small sky coverages or low sensitivities to highly-embedded objects attained so far limit their usefulness in revealing cluster structure. Submillimeter continuum images do reveal the most embedded objects but their relatively low resolutions preclude effective comparisons with near-infrared images. Interferometric millimeter observations of N_2H^+ 1–0 show a strong spatial coincidence with the submillimeter continuum objects, and can be used to trace radial velocities of this population at least. The Oph A filament shows small radial velocity dispersions, e.g., $\sim$0.2 km s^{-1}, at odds with predictions from some theories of cluster formation. The upcoming C2D and COMPLETE surveys of nearby star-forming molecular clouds will produce the sensitive, wide-field data needed to understand better the cluster formation process.

1. Introduction

Within nearby giant molecular clouds, 70-90% of young stellar objects (YSOs) are found within clustered environments (see Lada & Lada 2003 for an excellent review.) How such clusters form is not well understood. In recent years, many models of cluster formation have been proposed. The most popular constraints to these models have been the initial mass functions (IMFs) derived from observations of nearby embedded clusters. In general, recent models have been very successful in reproducing the power-law slope of the Salpeter IMF for masses above 1 $M_\odot$. Further constraints may be provided by comparing the predictions of models to the less well determined lower-mass end of the IMF (see paper by Luhman in this volume.) In this paper, we examine recent observations of the structures and kinematics of protoclusters, which could provide new constraints to models.

Embedded clusters have ages ranging from $<10^6$ yr to a few $\times$ 10^6 yr, with age spreads in their populations of the same order (Lada & Lada). Here we label the youngest embedded clusters as "protoclusters." Being very young, protoclusters contain a significant number of objects at a very embedded stage of protostellar evolution, i.e., preprotostellar cores (PPCs) and Class 0 objects. The protoclusters nearest to the Sun are those associated with the Ophiuchus star-forming region (distance = 125 pc; de Geus, de Zeeuw, & Lub 1989; de Geus 1992). Concentrating on the nearest examples of protoclusters maximizes the linear resolution of observational data and minimizes the incidence of foreground contamination, allowing the best insights into their populations. The recent catalogues of Porras et al. (2003) and Lada & Lada contain lists of all known embedded clusters within 1 kpc and 2 kpc respectively.

2. The Structures of Protoclusters

The structures of several embedded clusters have been determined through wide-field near-infrared imaging in recent years. Two types of structures have been observed. On the one hand, some clusters (e.g., NGC 2264) exhibit a hierarchical structure, i.e., several levels of clustering, possibly due to the hierarchical structure of the turbulent gas from which the clusters may have formed (Elmegreen et al. 2000). On the other hand, some clusters (e.g., IC 348, Trapezium-ONC) exhibit very centrally-concentrated structures, possibly due to the dominance of self-gravity on the cores from which they may have formed (Lada & Lada). The structures of embedded clusters, however, have been determined mostly from relatively old examples with ages of 1–2 $\times$ 10^6 yr. Too few clusters have been observed to get a real sense of how cluster structure may evolve with time.

Since protoclusters are relatively young, they represent an opportunity to glimpse the initial structure of embedded clusters, before substantial dynamical evolution of their populations occurs. Individual members can be very highly extincted, however, making it hard to recover the entire population of the protocluster. For example, Class 0 objects lie behind hundreds of magnitudes of visual extinction (André, Ward-Thompson, & Barsony 2000). It is therefore important at present to consider both wide-field, near-infrared imaging and submillimeter continuum mapping to include as much of a protocluster that can be detected when surveying its structure.

Figure 1 illustrates the limitations both near-infrared and submillimeter images have in displaying the structure of protoclusters. The Figure shows 850 μm continuum emission from the Oph A core observed by Wilson et al. (1999; see also Johnstone et al. 2000). Oph A contains a prominent continuum arc containing several PPCs and VLA 1623, the archetypical Class 0 object (André, Ward-Thompson, & Barsony 1993). Figure 1 also shows the positions of near-infrared objects detected from the surveys of Barsony et al. (1997; K_{lim} = 14.0) and Allen et al. (2002; H_{lim} = 21.0). (Note that all sources detected in these surveys are shown since no determinations of association with Oph A were made in these studies. The relatively high galactic latitude of Oph A, however, suggests there is relatively little contamination from background objects in the observed fields–see Allen et al.) The low sensitivity data of Barsony et al. show little clustering of objects about the Oph A field. The very sensitive observations of Allen et al., however, reveal a subcluster of objects $\sim$1.5$'$ to the east of the Oph A arc with a density rivalling that of the Trapezium, a clear example of what can remain hidden in the depths of extinction in such regions.

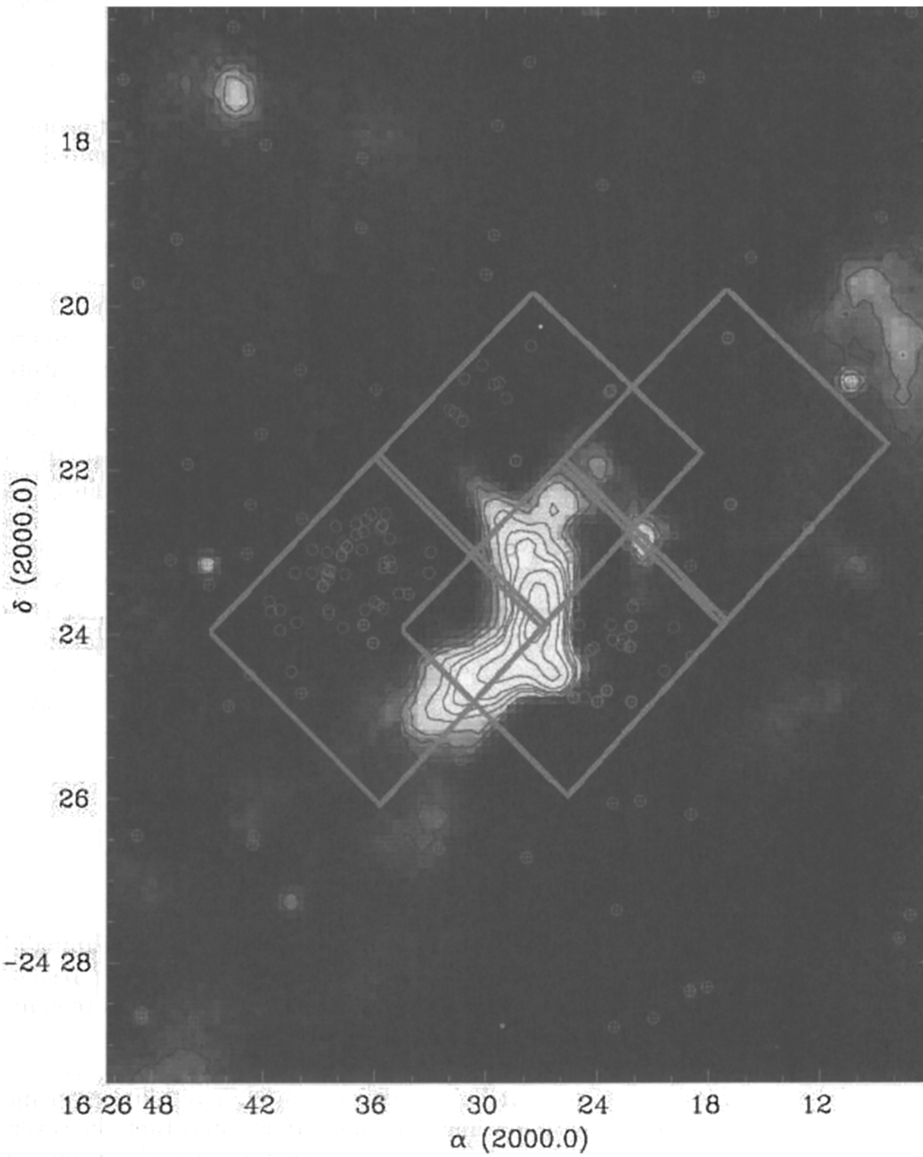

Figure 1. 850 μm continuum image of Oph A from Wilson et al. (1999; *greyscale*). Symbols indicate the positions of near-infrared objects found by Barsony et al. (1997; *crossed circles*) and Allen et al. (2002; *open circles*). The boxes show the edges of the Allen et al. survey only.

https://doi.org/10.1017/S0074180900241673 Published online by Cambridge University Press

Despite improvements in sensitivity and the corresponding hints of structure in Oph A, few near-infrared sources are actually found coincident with the bright 850 μm emission. Furthermore, the high sensitivity of the Allen et al. data was limited to a few, relatively small fields. (Note, for example, that the near-infrared objects in the dense subcluster are again found all the way to the eastern edge of the surveyed fields.) Submillimeter continuum maps do sample the very highly-embedded populations that near-infrared images so far cannot. The usefulness of such maps to reveal cluster structure, however, is limited by their relatively low resolution which can conceal objects with small angular separations and obfuscates the spatial relationships of more-embedded objects to the less-embedded population. In short, these limitations indicate numerous sources may still remain undetected within Oph A, making it difficult to say conclusively at present what its actual structure is.

For Oph A, it is tempting to speculate that the submillimeter continuum arc is physically related to the dense subcluster to the east, given that its curvature seems centered on the subcluster. Perhaps the combined winds and outflows from the subcluster have ploughed gas to the west into the arc of dense gas. (Such evidence is seen in the NGC 1333 protocluster region; see Knee & Sandell (1999) and Sandell & Knee 2000). The fact that new stars may be forming in these continuum objects suggests that protocluster structure may develop continually as the result of a succession of trigger events. Furthermore, it may be impossible to determine the initial conditions of cluster formation even from regions like Oph A, given that clustered star formation likely alters the surrounding core from the state when its first stars formed. Observations of regions in molecular cores with density enhancements but without signposts of star formation are clearly necessary to trace the evolution of the cloud core into stellar nurseries.

3. The Kinematics of Protoclusters

Other possible constraints for models of cluster formation are the velocity fields of the protoclusters. The kinematics of the near-infrared objects in Oph A, however, have not been measured. The sources in these regions are too faint to have their light dispersed to high enough spectral resolutions for meaningful kinematic analysis with present facilities (e.g., R=200000 for 1 km s^{-1} resolution). Tracing kinematics through the proper motions of these objects remains a possibility, but such an analysis of this region has not been published.

At their young age, protoclusters are still associated with dense gas, and the radial velocities of this gas can be determined at high resolutions using heterodyne instruments to detect its line emission. It is important, however, to choose a tracer of dense gas that is clearly associated with the youngest objects, given that different molecules have different excitation requirements and chemistries. For example, CO will deplete significantly in the dense, cold envelopes of PPCs and Class 0 objects. Fortunately, the N_2H^+ molecular ion remains abundant in gas at densities up to 10^{6-7} cm^{-3} (Aikawa, Ohashi, & Herbst 2003), and its 1–0 transition has a critical density of 2×10^5 cm^{-3}. Furthermore, the hyperfine structure of the 1–0 transition splits the line into 7 components, minimizing optical depth effects. Figure 2 demonstrates the clear coincidence of 850 μm continuum emission with N_2H^+ 1–0 emission, as detected

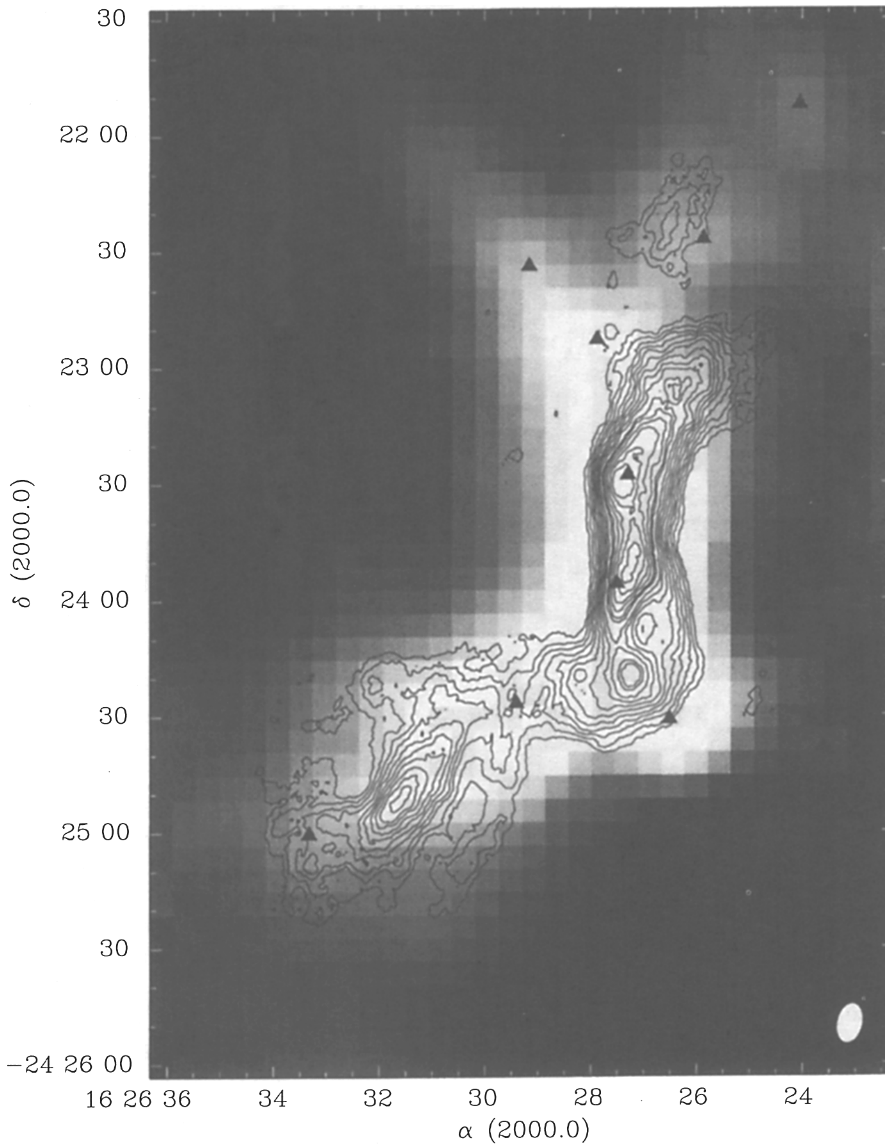

Figure 2. 850 μm image of Oph A from Wilson et al. (1999; *greyscale*) overlaid with the integrated intensity of N_2H^+ 1–0 emission from Di Francesco, André, & Myers (2003; *contours*). Symbols indicate the positions of submillimeter continuum objects detected by Motte, André, & Neri (1998; *triangles*). The ellipse in the lower right indicates the size of the synthesized beam FWHM of the N_2H^+ data.

by Di Francesco, André, & Myers (2003). (Note, however, the absence of N_2H^+ emission at the position of VLA 1623, possibly due to depletion onto grains at high densities or by its outflow.)

Figure 3 shows the radial velocities of dense gas in Oph A determined by fitting simultaneously all 7 components of N_2H^+ 1–0. The velocities have a very narrow range, with an rms of only $\sim$0.2 km s^{-1}, effectively the sound speed of Oph A at expected temperatures or less. Furthermore, the variations of radial velocities at the positions of the PPCs is minimal. This level of velocity coherence appears at odds with recent models of star formation in clustered environments where PPCs form via competitive accretion (e.g., Bonnell et al. 2001). Given the possible origin of the Oph A arc by external forces (see above), this may not be a general situation however. Observations of other protocluster regions (e.g, NGC 1333; see Walsh et al. 2003) are required to explore further this possibility.

4. The Near Future

Current observations of Ophiuchus, as well as similar data of other protoclusters like Serpens and NGC 1333 (in Perseus), suggest that no conclusive statements can be made about the structures and kinematics of protoclusters at the present time. Data from upcoming large-scale surveys, however, will provide much needed information. For example, the SIRTF Legacy project, "From Cores to Disks" (C2D), a large survey including near- and mid-infrared imaging of the entirety of Ophiuchus and 4 other nearby star-forming molecular clouds will begin in the coming year. These data will allow a census to be made of the cloud populations down to 0.001 $L_\odot$ (Evans et al. 2003), surpassing the limits of sensitivity and sky coverage seen in all previous infrared surveys of protocluster regions. In addition, the CO-ordinated Molecular Probe Line Extinction, and Thermal Emission (COMPLETE) survey, including wide-field mapping of the submillimeter continuum, millimeter line, and infrared extinction in Ophiuchus, Serpens, and Perseus has begun. An important consideration of both C2D and COMPLETE is that the data will have no proprietary time, and will be available widely and freely to the community. (For more about COMPLETE, see http://cfa-www.harvard.edu/COMPLETE.) Further down the road, wide-field, high-resolution submillimeter imaging by such instruments as ALMA will help constrain the structure and kinematics of the highly-embedded population at the same resolutions as infrared images. Such datasets, although large, will reveal the initial conditions of clusters, and bring us closer to understanding these important assemblages.

References

Aikawa, Y., Ohashi, N., & Herbst, E. 2003, ApJ, 593, 906

Allen, L. E., Myers, P. C., Di Francesco, J., Mathieu, R., Chen, H., & Young, E. 2002, ApJ, 566, 993

André, P., Ward-Thompson, D., & Barsony, M. 1993, ApJ, 406, 122

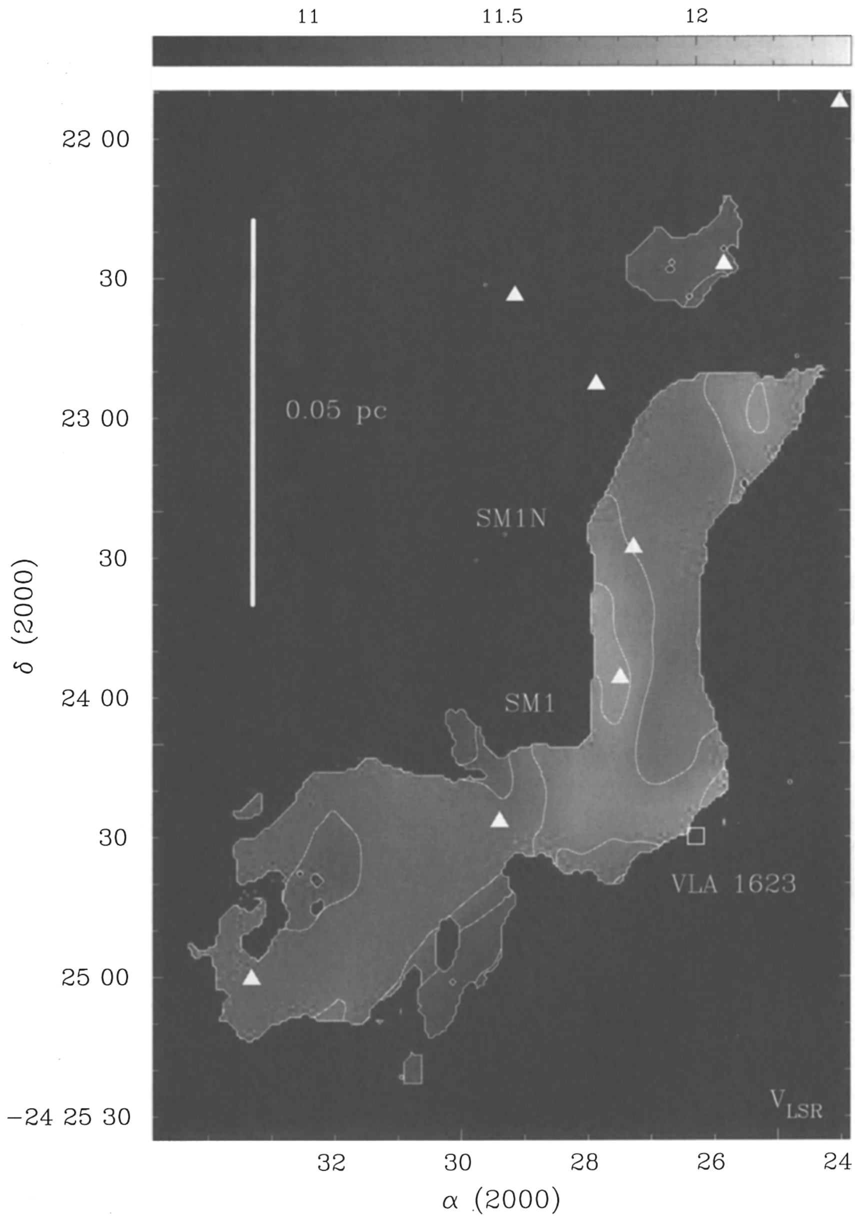

Figure 3. Map of V_{LSR} from N_2H^+ 1–0 across Oph A obtained by Di Francesco, André, & Myers (2003; *greyscale*). Contours represent steps of 0.2 km s^{-1}. Symbols denote the positions of submillimeter continuum objects detected in the region by Motte et al. (1998; *trangles* and *open square*).

https://doi.org/10.1017/S0074180900241673 Published online by Cambridge University Press

André, P., Ward-Thompson, D., & Barsony, M. 2003, in *Protostars and Planets IV*, eds. V. Mannings, A. P. Boss, & S. S. Russell, (Tucson: University of Arizona), p. 59

Barsony, M., Kenyon, S. J., Lada, E. A., & Teuben, P. J. 1997, ApJS, 112, 109

Bonnell, I. A., Bate, M. R., Clarke, C. J., & Pringle, J. E. 2001, MNRAS, 322, 859

de Geus, E. 1992, A&A, 262, 258

de Geus, E., de Zeeuw, P., & Lub, J. 1989, A&A, 216, 44

Di Francesco, J., André, P., & Myers, P. C. 2003, in preparation

Elmegreen, B. G., Efremov, Y., Pudritz, R. E., & Zinnecker, H. 2003, in *Protostars and Planets IV*, eds. V. Mannings, A. P. Boss, & S. S. Russell, (Tucson: University of Arizona), p. 179

Evans, N. J. II, et al., PASP, 115, 965

Johnstone, D., Wilson, C. D., Moriarty-Schieven, G., Joncas, G., Smith, G., Gregersen, E., & Fich, M. 2000, ApJ, 545, 327

Knee, L. B. G., & Sandell, G. 1999, A&A, 361, 671

Lada, C. J., & Lada, E. A. 2003, ARA&A, 41, 57

Motte, F., André, P., & Neri, R. 1998, A&A, 336, 150

Porras, A., Christopher, M., Allen, L. E., Di Francesco, J., Megeath, C. T., & Myers, P. C. 2003, AJ, in press

Sandell, G. & Knee, L. B. G. 2001, ApJ, 546, L49

Walsh, A. J., Di Francesco, J., Myers, P. C., Bourke, T. L., & Wilner, D. J. 2003, in preparation

Wilson, C. D., Avery, L. W., Fich, M., Johnstone, D., Joncas, G., Knee, L. B. G., Matthews, H. E., Mitchell, G. F., Moriarty-Schieven, G., & Pudritz, R. E. 1999, AJ, 513, L139